

The Location Optimization Problem of Urban Vertiports Based on Multimodal Transport

Jing Jiang¹, Yuzhen Guo^{1,*}, Junjie Yao¹ and Xuhui Wang²

¹ *School of mathematics, Nanjing University of Aeronautics Astronautics, Nanjing 211106, China*

² *China Academy of Civil Aviation Science and Technology, Beijing 100028, China*

Received 8 July 2025

Abstract. The facility location problem of urban vertiports is one of the crucial issues in urban low-altitude traffic optimization decisions. In order to effectively alleviate ground traffic congestion and improve passenger travel quality, this study focuses on the urban vertiport location optimization problem considering multi-modal transport. An integer programming model with capacity constraints and vertiport classification constraints is established. The model aims to minimize both vertiport construction cost and passenger travel cost. The RLT method is applied to linearize the non-convex quadratic terms in the objective function. For the reformulated optimal model, a depth-first branch-and-bound algorithm is developed. A branching strategy using priority functions is defined to enhance solving efficiency. Simulation experiments are conducted in the main urban area of Nanjing in China to verify the effectiveness of the model and algorithm. Three location schemes are proposed from the perspective of passenger, investor and bilateral equilibrium. Numerical results indicate that the bilateral equilibrium scheme is satisfied with both passenger travel demand and vertiport construction requirement. A comparative analysis of multimodal transport and ground traffic demonstrates that multimodal transport significantly reduces travel time while keeping cost increases within acceptable limits. These findings fully validate the feasibility and effectiveness of the proposed vertiport location scheme. The proposed schemes provide decision-making references for the strategic planning of urban air traffic infrastructure.

*Corresponding author.

Email: guoyuzhen@nuaa.edu.cn (Y. Guo)

AMS subject classifications: 90C10

Key words: Urban low-altitude traffic, urban vertiport, hub location problem, multimodal transport, branch-and-bound algorithm.

1 Introduction

With the rapid development of urbanization, traffic congestion and environmental pollution have become increasingly severe. In October 2016, Uber released a white paper introducing the concept of Urban Air Mobility (UAM) [1]. In 2018, the National Aeronautics and Space Administration (NASA) formally defined UAM as an air transportation system that provides efficient passenger and cargo transport services for urban areas through innovative aircraft, technologies and operations [2]. Electric Vertical Takeoff and Landing (eVTOL) aircraft offers some advantages such as vertical takeoff and landing capability, low noise emissions, environmental protection, etc. Utilizing eVTOL vehicles, UAM can provide faster, more efficient, greener transportation alternatives [3, 4]. Multimodal transport that combines air and ground transportation can fully tap the potential of low-altitude airspace and completely transform urban traffic conditions.

Vertiports are key infrastructure components of UAM networks. Their geographic location and internal design significantly affect operational capacity and service quality. Therefore, optimizing vertiport locations is crucial for the efficient deployment of future urban air mobility systems [5, 6]. This study focuses on the location optimization problem of urban vertiports based on multimodal transport.

Currently, methods for solving the vertiport location problem can be broadly classified into two categories: data-driven analysis and optimization modeling. Fadhil proposed a GIS-based method to determine vertiport locations for UAM systems [7]. Lim and Hwang applied the K-means clustering algorithm to select optimal vertiport locations and demonstrated its application along three major routes in Seoul [8]. Jeong et al. determined vertiport locations based on traveler demand and introduced noise-prioritized flight paths [9]. These studies are based on data analysis without establishing mathematical models. However, Holden and Goel developed a UAM network configuration model for Los Angeles and London, using clustering algorithm to assign demand to discrete candidate locations [1]. Daskilewicz et al. formulated a vertiport location model assuming all urban UAM trips are within 30 miles. This model neglected infrastructure construction cost and capacity constraints [10]. Rath and Chow introduced a hub location model incorporating user

choice behavior constraint. It was tested in New York City [11]. Chen et al. proposed a discrete vertiport location model based on grid partitioning excluding unsuitable areas. They further developed a variable neighborhood search-based heuristic to solve the mathematical formulation [12]. Shin et al. presented an optimization model that considers traffic congestion, minimizing travel time, vertiport construction cost, service cost and collision risk. They proposed a genetic algorithm based on two-dimensional chromosomes to solve it [13]. Wei et al. incorporated capacity as a constraint in vertiport location selection but their model focused exclusively on high-demand zones [14]. Zhang et al. established an integer programming model aiming to minimize total economic cost while maximizing customer satisfaction [15]. Based on the location problem of urban vertiports, this study will adopt an optimization modeling method and take into account factors such as vertiport construction cost, passenger travel expenses.

O'Kelly [16] first proposed the mathematical model of the Hub Location problem (HLP), which is a quadratic model. Campbell [17] was the first to transform the hub location model into a linear integer programming model. Sangaiah et al. argued that optimizing hub network configurations and resource allocation can significantly reduce transportation cost, enhance system reliability and generate substantial economic benefits [18]. Wandelt et al. conducted large-scale benchmark experiments to evaluate and compare four standard exact algorithms across 12 HLP instances, offering new insights and experimental basis for solving such problems [19]. Alumur et al. suggested addressing the hub effect in the HLP model, that is, the congestion between hubs caused by the high service demands of hub nodes. The direct way to solve the congestion is to explicitly introduce cost terms related to congestion in the objective function or add capacity constraints [20]. Najy and Diabat proposed an HLP model that incorporates congestion cost into the objective function to reflect the negative impacts of scale-induced congestion [21]. Therefore, this study builds an HLP-based model for the vertiport location problem by considering multimodal transportation, capacity constraints and vertiport level.

2 Vertiport Location Model

2.1 Problem Description

The multimodal urban transportation system incorporating air mobility consists of three segments: ground transport from the origin to the vertiport, aerial travel via eVTOL between departure/arrival vertiports, ground transport from the arrival vertiport to the destination, as illustrated in Figure 1. Vertiports act as hub nodes connecting demand points; therefore, the vertiport location problem is formulated as

a hub location problem in this paper. Kreimeier et al. thought that willingness-to-pay for air mobility services is significantly affected by the distance of ground access, with users tending to select the nearest vertiport [22]. Hence, a single-assignment model is adopted in this paper. Additionally, vertiport level and capacity on location decisions are considered.

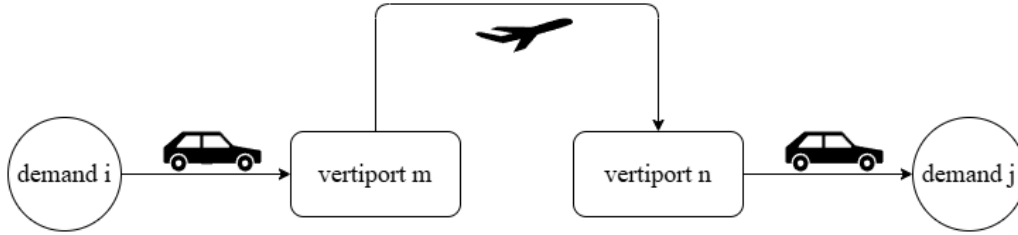


Figure 1: Schematic diagram of multimodal transport

Based on service volume, vertiports are categorized into three levels:

(1) Vertihub: As the core infrastructure of UAM networks, it provides takeoff, landing and parking services for eVTOLs. Each city must have at least one vertihub, which serves the highest passenger volume.

(2) Vertiport: A primary facility for eVTOL operations, capable of accommodating a small number of aircraft simultaneously. It serves a moderate passenger volume.

(3) Vertistop: The smallest type of vertiport, typically equipped with one or two landing pads without parking spaces, serving the lowest passenger volume.

2.2 Model Formulation

Based on the location problem of urban vertiports, we aim to minimize the total cost, including vertiport construction cost and passenger travel cost, while satisfying all travel demands and vertiport capacity limits. The optimization model P is formulated as follows:

$$\begin{aligned} \min & \theta_1 \left(\sum_{m \in H} \sum_{k \in K} f_k z_{mk} \right) + \theta_2 \left(\sum_{i \in N} \sum_{j \in N} \delta \omega_{ij} \left(\sum_{m \in H} d_{im} y_{im} + \sum_{n \in H} d_{jn} y_{jn} \right) \right) \\ & + \sum_{i \in N} \sum_{j \in N} \zeta \omega_{ij} \left(\sum_{m \in H} \sum_{n \in H} D_{mn} y_{im} y_{jn} \right) \end{aligned} \quad (1)$$

$$\text{s.t. } \sum_{m \in H} y_{im} = 1, \quad \forall i \in N, \tag{2}$$

$$\sum_{k \in K} z_{mk} \leq 1, \quad \forall m \in H, \tag{3}$$

$$y_{im} \leq \sum_{k \in K} z_{mk}, \quad \forall i \in N, m \in H, \tag{4}$$

$$\sum_{i \in N} \sum_{j \in N} \omega_{ij} y_{im} \leq \sum_{k \in K} a_k z_{mk}, \quad m \in H, \tag{5}$$

$$y_{im} \in \{0, 1\}, \quad i \in N, m \in H, \tag{6}$$

$$z_{mk} \in \{0, 1\}, \quad m \in H, k \in K, \tag{7}$$

where θ_1 and θ_2 are weight coefficients for the two objectives, which are simply varied in the sensitivity analysis as exogenous parameters; H is the set of candidate vertiport locations, m, n are the indexes of the candidate vertiports; N is the set of demand points (including origins and destinations), i, j are the indexes of the demand points; K is the set of vertiport levels, k represents the level of vertiport, $k=0, 1, 2$ denotes vertistop, vertiport and vertihub respectively; f_k is the construction cost of k level vertiport; a_k is the capacity of k level vertiport, a_0, a_1 , and a_2 correspond respectively to vertistop, vertiport, and vertihub, their values are given later in Table 1; ω_{ij} is the travel demand between demand points i and j ; d_{im} is the distance from demand point i to vertiport m ; D_{mn} is the distance between vertiports m and n ; δ is the unit distance cost for ground travel; ζ is the unit distance cost for air travel; y_{im} is the decision variable, 1 if demand point i is served by vertiport m , 0 otherwise; z_{mk} is the decision variable, 1 if vertiport m is k level, 0 otherwise.

In Equation (1), the first term represents the total vertiport construction cost, the second term accounts for passenger ground transportation cost and air travel cost. $(\sum_{m \in H} d_{im} y_{im} + \sum_{n \in H} d_{jn} y_{jn})$ presents ground distance from demand point i to vertiport m and from vertiport n to demand point j . $\sum_{m \in H} \sum_{n \in H} D_{mn} y_{im} y_{jn}$ presents air distance between vertiport m and vertiport n . Constraint (2) ensures that each demand point is assigned to exactly one vertiport. Constraint (3) guarantees that at most one level of vertiport is selected at each candidate location. Constraint (4) ensures that no unestablished candidate location serves any demand. Constraint (5) imposes capacity limits on each selected vertiport. Constraints (6) and (7) define all decision variables as binary.

2.3 Model Reformulation

The second term in the objective function contains the nonlinear term, making the problem difficult to solve. The Reformulation-Linearization Technique (RLT) is applied to linearize it. Let $x_{ijmn} = y_{im}y_{jn}$, which is a new variable indicating 1 if demand pair i, j is connected via vertiports m, n , and 0 otherwise. This new variable is 1 only if y_{im} and y_{jn} are all 1; otherwise, it is 0. Therefore, the following constraints are introduced:

$$x_{ijmn} \leq y_{im}, \quad \forall i, j \in N, m, n \in H, \quad (8)$$

$$x_{ijmn} \leq y_{jn}, \quad \forall i, j \in N, m, n \in H, \quad (9)$$

$$x_{ijmn} \geq y_{im} + y_{jn} - 1, \quad \forall i, j \in N, m, n \in H, \quad (10)$$

$$x_{ijmn} \in \{0, 1\}, \quad i, j \in N, m, n \in H. \quad (11)$$

An integer programming model \bar{P} is obtained after reformulating by the RLT, with x_{ijmn} , y_{im} , and z_{mk} as decision variables, as follows:

$$\begin{aligned} \min \quad & \theta_1 \left(\sum_{m \in H} \sum_{k \in K} f_k z_{mk} \right) + \theta_2 \left(\sum_{i \in N} \sum_{j \in N} \delta \omega_{ij} \left(\sum_{m \in H} d_{im} y_{im} + \sum_{n \in H} d_{jn} y_{jn} \right) \right) \\ & + \sum_{i \in N} \sum_{j \in N} \zeta \omega_{ij} \sum_{m \in H} \sum_{n \in H} D_{mn} x_{ijmn} \\ \text{s.t.} \quad & (2) - (7), (8) - (11). \end{aligned} \quad (12)$$

In the model \bar{P} , the objective function and constraint functions are linear, x_{ijmn} , y_{im} and z_{mk} are integer variables.

3 Algorithm Design

The branch-and-bound algorithm is an exact method for solving integer programming problems. Its core idea involves relaxing integer variables to continuous ones, solving the resulting linear relaxation, then selecting a non-integer variable x_i^* from the solution vector \bar{x}^* . The original problem is split into two subproblems by adding branching constraints $x_i \leq \lfloor x_i^* \rfloor$ and $x_i \geq \lceil x_i^* \rceil$. By iteratively solving these subproblems, the search space is progressively narrowed through updates of upper and lower bounds, while portions of the solution space that cannot yield an optimal solution are pruned, thereby improving the efficiency of the search for the global optimum.

However, for large-scale problems, the computational speed of the standard branch-and-bound algorithm can be relatively slow. To address this limitation,

Samir M. et al. proposed a high-complexity branch-and-reduce algorithm tailored for mixed-integer programming [23]. Oliveira F.A. et al. improved the efficiency of the branch-and-bound framework for profit-maximizing multi-allocation hub network design by incorporating Benders decomposition and Pareto-optimal cuts [24]. Yin J. et al. formulated an integer programming model for train rescheduling in urban rail transit systems and solved it using a depth-first branch-and-price algorithm [25].

As the problem size increases, certain branching decisions may have minimal impact on tightening the upper and lower bounds, leading to numerous ineffective branches. In contrast, depth-first search can rapidly generate feasible integer solutions, thus improving the convergence of the upper bound. With increasing demand points, the scale of \bar{P} expands significantly. To achieve rapid and effective solutions, this study employs a depth-first branch-and-bound algorithm.

To further accelerate the algorithm, this study introduces a priority-based branching rule based on the linear relaxation solution. For each non-integer variable x_i^* in the solution x^* , rounding up and rounding down while keeping other variables fixed creates new solutions x_i^+ and x_i^- . The corresponding objective values are denoted as z_i^+ and z_i^- , respectively. Let z^* represents the objective value of the current linear relaxation solution x^* . The increments of the objective function are defined as $\Delta_i^+ = |z_i^+ - z^*|$ and $\Delta_i^- = |z_i^- - z^*|$. These increments are approximately calculated through pseudo-cost. The priority expression for this variable is defined as $\min\{\Delta_i^+, \Delta_i^-\}$. The non-integer variable with the highest priority is selected for branching:

$$i = \operatorname{argmax}\{\min\{\Delta_i^+, \Delta_i^-\}\}.$$

For the reformulated integer programming model \bar{P} , we employ a branch-and-bound algorithm incorporating priority and depth-first strategies. The algorithm flow is as follows:

Step 1: Initialization. Place the linear relaxation problem P_0 of the original problem \bar{P} into the problem set T to be solved. Set the current best objective value $z^* = +\infty$.

Step 2: Check if T is empty, stop and output z^* , x^* . Otherwise, proceed to Step 3.

Step 3: Solve the last problem P_k in T . If infeasible, remove P_k from T , then return to Step 2. Otherwise, obtain solution x_k and objective value z_k .

Step 4: Compare z_k with z^* . If $z_k \geq z^*$, remove P_k from T , then return to Step 2. If $z_k < z^*$, check if all variables in x_k are integers, set $z^* = z_k$ and $x^* = x_k$, remove P_k from T , then return to Step 2. Otherwise, proceed to Step 5.

Step 5: Based on the priority function of non-integer variables, decompose problem P_k into two subproblems P_{k+1} and P_{k+2} . Remove P_k from T . Add P_{k+1}

and P_{k+2} to the end of T . Return to Step 2.

In Step 5, prioritized branching is implemented by decomposing the problem based on priority. The depth-first search strategy is implemented by adding the new subproblems to the end of the set T and always selecting the last problem in Step 3.

4 Numerical Experiments

For the urban air mobility vertiport location problem, numerical experiments were conducted in the main urban area of Nanjing City (Xuanwu District, Qinhuai District, Jianye District, Gulou District, Qixia District, and Yuhuatai District). The experimental environment was configured with an Intel(R) Core(TM) i7-10750H CPU @ 2.60GHz, 16.00GB RAM, running Windows 10 (64-bit).

4.1 Demand Points and Vertiport Candidate Locations

Regarding travel demand, existing ground transportation stations in Nanjing, namely bus stops and subway stations, were acquired. The main urban area has 2197 bus and subway stations. The locations of these stations inherently reflect the physical mapping of urban population distribution and travel demand. Station distribution is naturally concentrated in high-activity urban areas: residential zones, office areas and commercial districts which exhibit high station density, indicating greater potential demand for multimodal travel in these regions. Station passenger flow data directly reflects the spatiotemporal distribution characteristics of regional travel demand, providing dynamic references for urban air mobility. Simultaneously, using ground transport stations as origin demand nodes aims to construct a ground-air multimodal transport network. Coupling vertiport locations with bus and subway stations can reduce user transfer distances, for example, by utilizing open spaces or rooftops near stations as landing platforms to achieve "last-mile" connectivity. From a data availability perspective, bus and subway station locations and passenger flow data are publicly available and systematized, serving as reliable inputs for air mobility demand modeling. Therefore, bus and subway stations are considered as origin demand points.

This study first clusters these origin demand points into k demand centers using the K-means algorithm. According to Mardia et al.'s empirical rule, a suitable k is a function of sample size n , $k \approx \sqrt{n}/2$ [26]. Therefore, the number of demand centers was set to approximately 30. Travel demand between each pair of demand centers is then allocated proportionally based on the number of origin points contained within each demand center.

Lim and Hwang proposed using the K-means clustering algorithm to directly select vertiport locations [8]. As clustering is inherently heuristic, we first use K-means to determine candidate vertiport locations, then employs the optimization model to finalize the selection. Jeong et al. [9] selected 100 candidates for a population of 21 million. Considering the main urban area's population of 3.3468 million according to census data, 16 candidate points were set and identified using the K-means algorithm.

4.2 Parameter Setting

The ground transport cost per kilometer between demand point and vertiport was set at 3 Chinese Yuan (CNY)/km*, referencing Nanjing taxi and online ride-hailing fare standards. For air travel, based on statements by Shanghai Autoflight Co., Ltd., the eVTOL fare per kilometer per person is projected to reach 6 CNY/km†.

Based on data from reference [27], construction cost and daily capacity parameters for the three vertiport levels were set as shown in Table 1.

Table 1: Vertiport parameters

Level	Construction cost/million yuan	Daily capacity of the vertiport
vertihub	4000	2000
vertiport	2400	1000
vertistop	1680	600

4.3 Numerical Results

The main urban area of Nanjing (Xuanwu, Qinhuai, Jianye, Gulou, Qixia, Yuhuatai districts) has 2197 bus and subway stations. Using the K-means algorithm, 30 demand points and 16 candidate vertiport locations were generated, as shown in Figure 2. Small black dots represent bus/subway stations, large green dots represent demand points, five-pointed star icons represent candidate vertiports. Areas with dense ground stations correspond to higher concentrations of demand points and candidate vertiports, such as the central districts (Xuanwu, Qinhuai, Jianye, Gulou). Areas with sparse stations also have demand points and candidates but the number is small, such as the southwest (Yuhuatai) and north (Qixia) regions in Figure 2. Table 2 shows the total travel demands starting from each demand point.

*https://fgw.nanjing.gov.cn/njsfzhggwyh/202501/t20250124_5065713.html

†<https://www.stcn.com/article/detail/1287022.html>

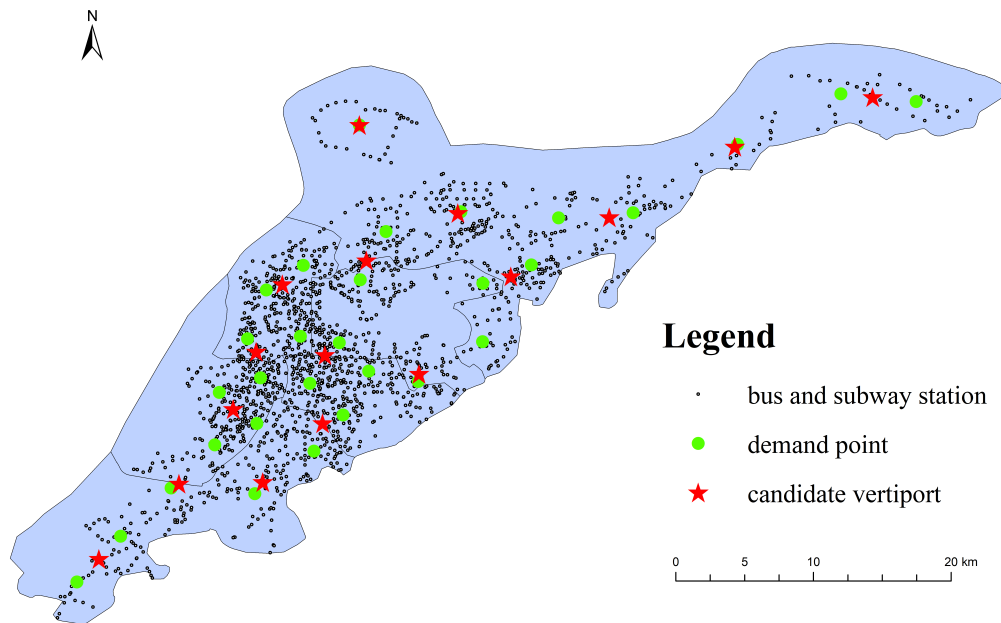


Figure 2: demand points and candidate vertiports in Nanjing main urban area

Table 2: The demand value of the demand point(number of trips)

No.	0	1	2	3	4	5	6	7	8	9	10	11	12	13	14
demand	359	132	335	69	468	353	147	125	397	107	286	189	198	198	340
No.	15	16	17	18	19	20	21	22	23	24	25	26	27	28	29
demand	409	338	250	301	286	256	56	289	171	259	84	448	364	298	46

Table 3 provides the longitude, latitude and detailed location of the 16 candidate vertiport sites. All sites possess suitable conditions for vertiport construction.

Yuhuatai District People’s Government (Candidate 0): This site is suitable for dedicated facilities for government emergency command, addressing the requirement for rapid response to public incidents. Taipingshan Park (Candidate 1), Xianhemen Park (Candidate 12) and Yuhua Urban Park (Candidate 15): These locations feature open spaces suitable for constructing vertiports, serving surrounding communities. Jiangsu Provincial Hospital of Integrated Traditional Chinese and Western Medicine (Candidate 2), Nanjing Qixia Xiehe Senior Service Center (Candidate 8), and Nanjing Gulou Gangtai Hospital of Traditional Chinese Medicine (Candidate 10): These candidate sites offer potential to support cross-regional deployment, transfer and transport capabilities for critical medical supplies. Nanjing Olympic

Sports Center (Candidate 3): The venue’s roof and plaza provide ample landing and takeoff space. Additionally, transport capacity can be significantly enhanced during major events. Longtan Station (Candidate 4): As a railway freight yard, this site presents an opportunity for conversion into a logistics-oriented eVTOL hub, facilitating "air-rail intermodal" operations. Yuhuatai Special Education School (Candidate 5): Potential exists for site conversion utilizing the school’s playground or rooftop areas. Nanjing Agricultural University (Weigang Campus) (Candidate 6) and Nanjing University (Xianlin Campus) (Candidate 11): As higher education institutions, these sites can utilize open campus areas for vertiport construction, serving inter-university academic exchanges or commuting for high-end talents. Xinjiekou Commercial District (Candidate 7): This location features multiple high-rise buildings exceeding 200 meters. Demand for premium business travel and instant logistics services here is very strong. Here, vertiport operations could be enhanced through seamless integration with the metro system. Changgou Road Guzhuang, Qixia District (Candidate 13): The low population density characteristic of this suburban location makes it suitable for establishing logistics service base stations. Tianbao Metro Station (Candidate 14): This site can serve commuting demand for the Jiangbei New District, contributing to the alleviation of ground traffic pressure.

Table 3: Candidate vertiport location

No.	Longitude	Latitude	Location
0	118.786035	31.999178	Yuhuatai District People’s Government
1	118.874378	32.136491	Taipingshan Park
2	118.814658	32.105528	Jiangsu Provincial Hospital of Integrated Traditional Chinese and Western Medicine
3	118.7276	32.008402	Nanjing Olympic Sports Center
4	119.055378	32.179777	Longtan Station
5	118.639921	31.910669	Nanjing Yuhuatai District Special Education School
6	118.849051	32.031488	Nanjing Agricultural University (Weigang Campus)
7	118.787529	32.043772	Xinjiekou Business District
8	118.810084	32.193968	Nanjing Qixia Xiehe Senior Service Center
9	118.742634	32.045941	Wuyue Plaza (Nanjing Jianye Branch)
10	118.759757	32.090017	Nanjing Gulou Antai Traditional Chinese Medicine Hospital
11	118.973412	32.133715	Nanjing University (Xianlin Campus)
12	118.90905	32.095084	Xianhemen Park
13	119.145455	32.21219	Guzhuang, Changgou Road, Qixia District, Nanjing City
14	118.692198	31.959703	Tianbao Subway Station
15	118.746924	31.960784	Yuhua City Park

4.3.1 Sensitivity Analysis

The model’s objective function comprises two main components: vertiport construction cost and travel cost, weighted by coefficients θ_1 and θ_2 . The impact of these weights on the results is first explored. θ_1 was varied from 0.1 to 0.9, while θ_2 varied inversely from 0.9 to 0.1, ensuring $\theta_1 + \theta_2 = 1$.

The experimental environment was configured with an Intel(R) Core (TM) i7-10750H CPU @ 2.60GHz, 16.00GB RAM, running Windows 10 (64-bit). The average CPU time of the 16 candidate vertiports network is 423.56 seconds.

Figure 3 shows that as the construction cost weight coefficient θ_1 increases, the total number of vertiports shows a downward trend. When $\theta_1 = 0.1$, the focus is minimizing passenger travel cost, leading to the maximum number of vertiports, distributed across all six districts. When $\theta_1 = 0.9$, the minimum number of vertiports is 7, including 2 vertihubs, 3 vertiports and 2 vertistops. Because at this time, under the premise of meeting the capacity limit, the construction cost is guaranteed to be the minimum, while the travel cost of passengers is ignored. In this case, all vertiport levels are concentrated in high-demand areas, as shown in Figure 4(i). For other values of θ_1 , the number of vertiports is shown in Figure 3. Figures 4 (a)-(i) show that θ_1 increases from 0.1 to 0.9, the vertiports become increasingly concentrated in high-demand areas.

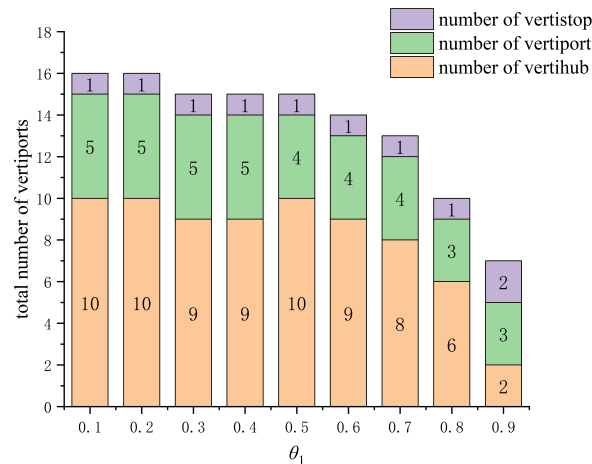


Figure 3: Number of Vertiport

As shown in Figure 5 and Table 4, increasing the construction cost weight coefficient θ_1 leads to reduced construction cost but increased travel cost. The total cost first decreases, then increases, reaching its minimum to approximately 957.36 million CNY when $\theta_1 = 0.5$.

From the perspective of vertiport utilization rate, it is defined as vertiport passenger flow divided by its capacity in this paper. A low vertiport utilization rate indicates underutilized resources, while a high rate indicates potential congestion. As shown in Figure 6, the utilization rate increases from 58% to 92% as θ_1 increases. Although the utilization rate is highest when $\theta_1 = 0.9$, the number of vertiports is

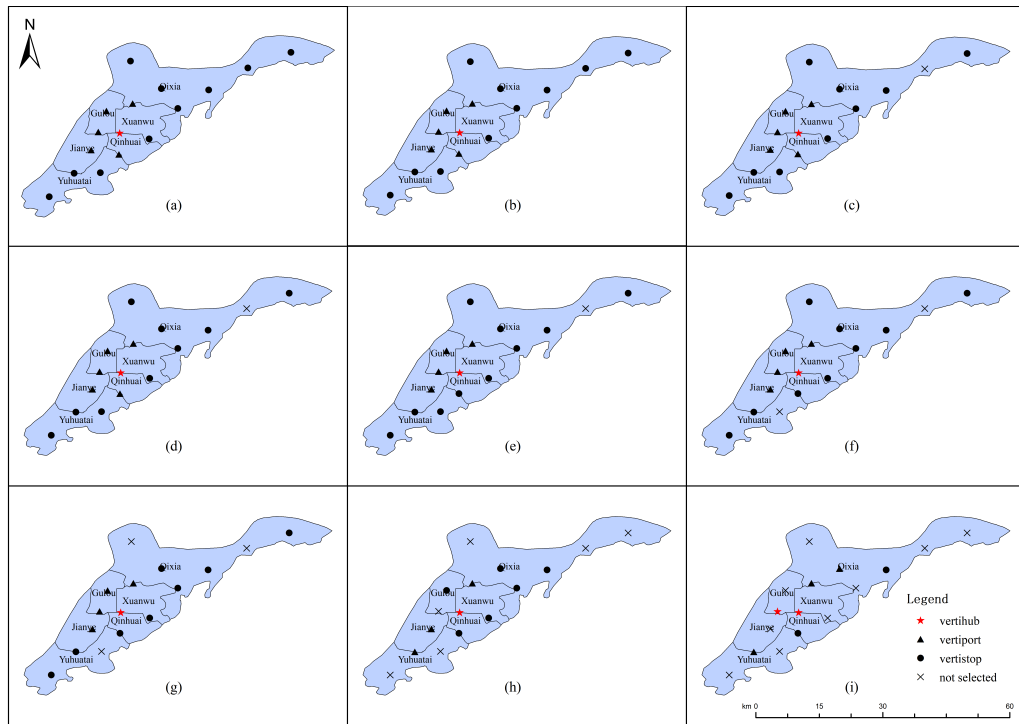


Figure 4: Vertiport Location under different θ_1 value

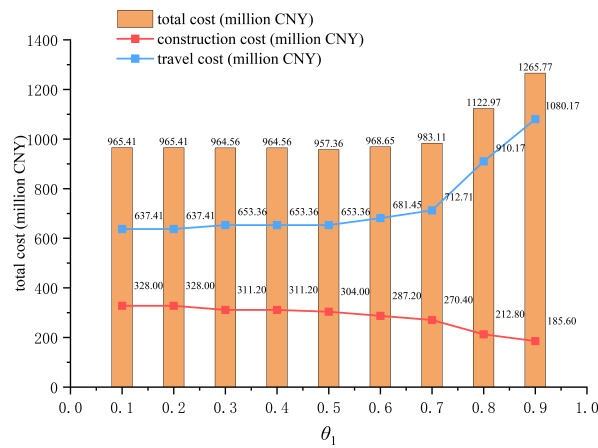


Figure 5: Vertiport Location under different θ_1 value

minimal, inevitably leading to congestion as the city develops.

This study provides diversified vertiport deployment schemes. From the passen-

Table 4: Vertiport Location decision under different θ_1

θ_1	Total cost/ million CNY	construction cost/ million CNY	Travel cost/ million CNY
0.1	965.41	328.00	637.41
0.2	965.41	328.00	637.41
0.3	964.56	311.20	653.36
0.4	964.56	311.20	653.36
0.5	957.36	304.00	653.36
0.6	968.65	287.20	681.45
0.7	983.11	270.40	712.71
0.8	1122.97	212.80	910.17
0.9	1265.77	185.60	1080.17

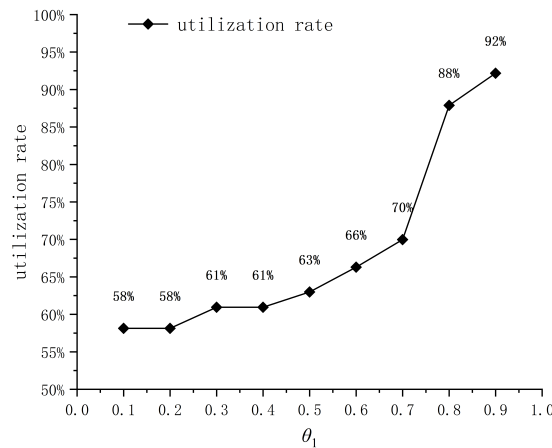


Figure 6: Utilization rate of vertiport

ger interest perspective, the weighting coefficient θ_1 should be set at 0.1 or 0.2, corresponding to a "Build as much as possible" strategy for vertiports. This approach reduces travel cost, mitigates congestion and elevates service levels. Compared to the scheme with $\theta_1=0.9$, it achieves a travel cost reduction of RMB 442.76 million, with a reduction rate of 41%. Although this scheme yields a vertiport utilization rate of only 58%, it strategically allocates development space within public transportation planning. However, urban development and rising living standards will lead to increased demand for air travel, so public transportation planning should reserve room for future growth. Conversely, from the investor perspective, the scheme with $\theta_1=0.9$ is recommended under the premise of meeting travel demand. This configuration reduces construction cost by RMB 142.40 million compared to the $\theta_1=0.1$ scheme, with a reduction rate of 43.41%. From the bilateral equilibrium perspec-

tive, the optimal scheme employs $\theta_1=0.5$. This equilibrium solution minimizes total cost while achieving 63% utilization rate, thereby avoiding resource underutilization while retaining sufficient capacity for future demand growth.

4.3.2 Location Scheme Determination

Based on the analysis presented in the preceding section, we adopt the bilateral equilibrium perspective by selecting the vertiport location scheme corresponding to $\theta_1=0.5$. This optimal configuration yields a total cost of approximately RMB 957.36 million, representing the minimum expenditure across all scenarios. The breakdown comprises construction cost of RMB 304 million and travel cost (calculated based on 365 days of demand) amounting to RMB 653.36 million. The scheme entails establishing 15 vertiports with a utilization rate of 63%, as detailed in Table 5.

Table 5: Vertiport Location decision

Total cost/ million CNY	957.36
construction cost/ million CNY	304.00
Travel cost/ million CNY	653.36
total number of vertiports	15
number of vertihub	1
number of vertiport	4
number of vertistop	10

The spatial distribution of vertiports is illustrated in Figure 7 under the $\theta_1=0.5$ scheme. The vertihub is centrally positioned within the main urban core, encircled by 4 vertiports. 10 vertistops are strategically located along the periphery to provide supplementary coverage. Specifically, the vertihub is situated within the Xinjiekou Commercial District—Nanjing’s highest traffic volume zone. This location features numerous flat-roofed buildings exceeding 200 meters in height, including Deji Plaza, the Jinling Hotel Asia-Pacific Business Tower, Jinling Central, Nanjing International Financial Center and Golden Eagle International Mall, rendering it exceptionally suitable for vertihub infrastructure.

Vertiport locations are specified as follows:

Vertiport 2: Located at Jiangsu Provincial Hospital of Integrated Traditional Chinese and Western Medicine (at the border of Qixia and Xuanwu Districts), featuring a 23-story main building and 11-story auxiliary structure.

Vertiport 3: Located at Nanjing International Financial Center, proximate to Nanjing Olympic Sports Center.

Vertiport 9: Sited at Wuyue Plaza (Nanjing Jianye).

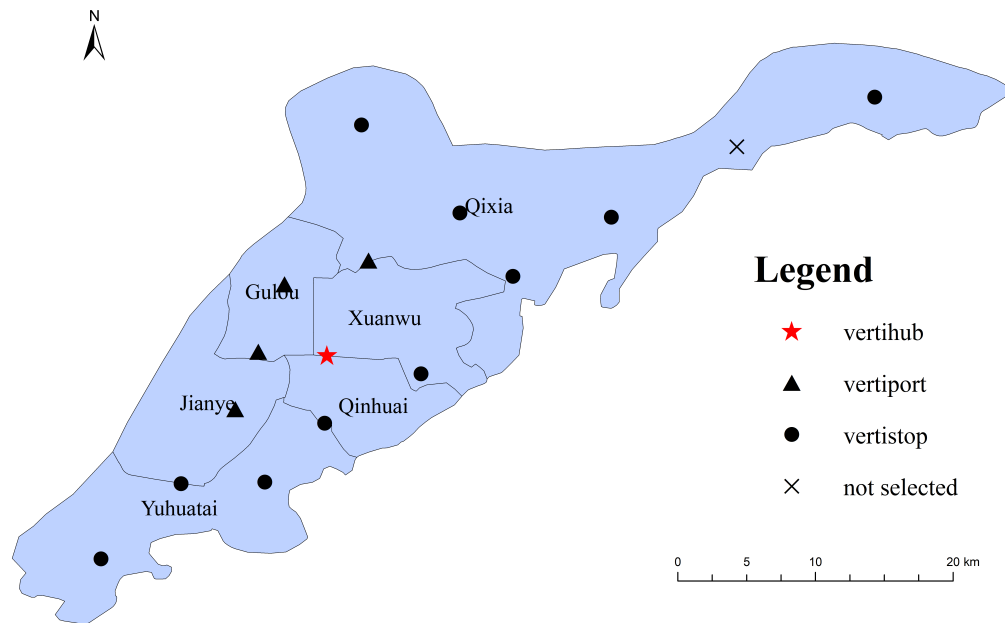


Figure 7: Vertiport Location

Vertiport 10: Positioned at Nanjing Gulou Gangtai Hospital of Traditional Chinese Medicine.

All selected sites occupy strategic positions within commercial centers, healthcare facilities and office complexes. These locations inherently prioritized for vertiport development, demonstrating the scheme's strong practical feasibility.

4.3.3 Comparing multimodal transport with ground transportation

To analysis the cost and time of multimodal transport including air transportation and ground transportation, 10 pairs of travel OD are randomly generated to calculate the cost and time required for directly taking ground transportation and multimodal transport from the starting point to the destination j respectively, as shown in Table 6. Among them, the travel mode of ground transportation is taxi, its cost and time are obtained from the Amap taxi software. The cost and time of multimodal transport are calculated by the model in this study. As is known from Table 6, the cost of multimodal transport including air traffic is mostly about twice that of ground transportation, the time spent is reduced by more than 40 percent. As in Example 6, the travel time has been reduced from 37 minutes to 7 minutes, a decrease of 80% of the travel time. In Example 4, it has been reduced from 67

minutes to 24 minutes, which is of positive significance for passengers with a high time value bias. As for Example 5, the travel time was only shortened by 30%. Since the taxi travel time is relatively short, the taxi fare at this time is half of the multimodal transport fare. Therefore, the multimodal transport of this type is not attractive enough to passengers. For Example 2 and Example 3, the travel distances are almost the same, the multimodal transport cost vary greatly. The multimodal transport price of Example 2 is 1.6 times that of Example 3. Through analysis, it is found that the starting point and destination of Example 2 are between two vertiports, as shown in Figure 8, which leads to a longer flight distance in the air and high cost. However, the travel time of multimodal transport is half that of taxi travel. Therefore, passengers can choose their own travel mode according to their own needs.

Table 6: Comparison between ground transportation and multimodal transport

example	denand i	vertiport m	vertiport n	demand j	Distance /km	taxi cost /CNY	taxi time /min	multipodal transport cost/CNY	multipodal transport time/min
1	4	7	3	16	5.14	22	17	51.88	9
2	6	5	15	13	8.84	26	19	78.54	10
3	8	9	0	19	9.11	35	20	49.14	9
4	5	1	11	23	10.62	33	22	61.26	7
5	7	6	10	14	12.37	41	24	83.18	16
6	18	6	8	9	18.93	57	37	112.02	7
7	11	12	3	2	22.51	59	32	128.66	14
8	10	0	11	21	31.23	116	57	171.61	30
9	26	7	13	29	42.60	129	54	246.44	23
10	12	14	13	29	53.81	156	67	316.67	24

5 Conclusion

Regarding the location problem of urban vertiports, based on the hub location model, this study aims to minimize construction costs and travel expenses considering the selection of vertiport levels and capacity constraints. For the nonlinear terms in the objective function, this study adopts the RLT to linearize them. The model is reconstructed into an integer programming model. To solve the reformulated model, we construct the branch priority function, then use the depth-first branch and bound algorithm.

This study conducts a simulation experiment in the main urban area of Nanjing City. The transportation stations in Nanjing City are clustered to obtain the data of demand points. The experimental results show that the model proposed in this study is highly feasible. The selected locations include shopping centers, hospitals,

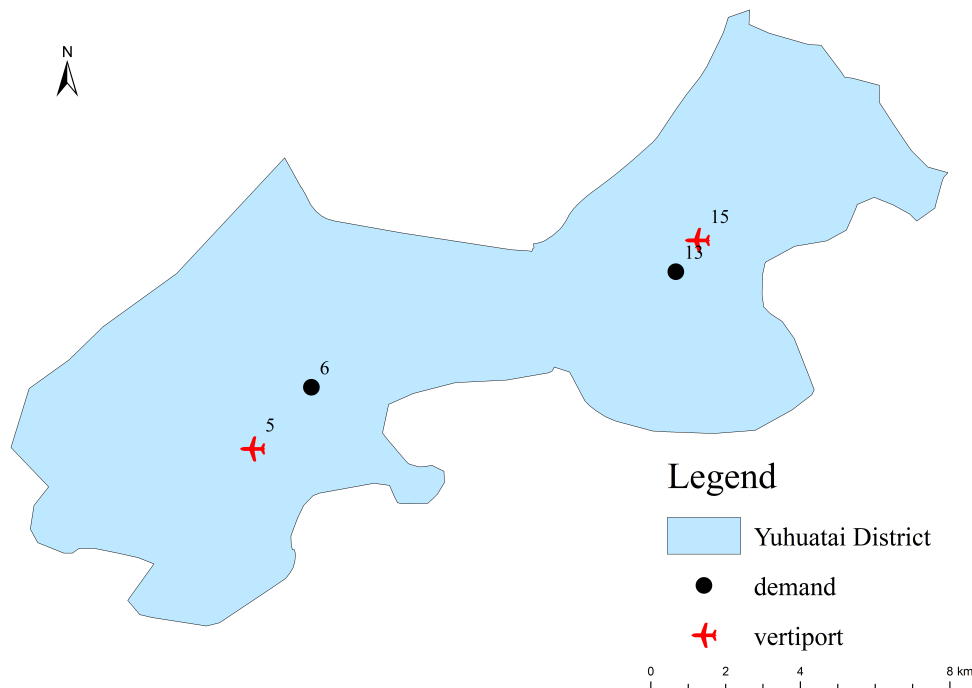


Figure 8: The locations of OD and the vetriports in Example 2

office buildings, etc., which are suitable for building vertiports. The research content can provide solutions for the layout of projects such as urban vertiports and urban air taxis. Appropriate strategies for different decision-makers can be offered.

Future research work can comprehensively consider factors such as population, GDP and income level to select candidate sites. It can also further consider the location selection of vertical take-off and landing points in the case of uncertain travel demand. The numerical experiment can be extended to Nanjing City and surrounding cities for the research of large-scale integrated vertiport location schemes. Meanwhile, heuristic algorithms can be adopted to deal with the solution of large-scale problems.

Acknowledgments

This work was supported by the General Programs of National Natural Science Foundation of China (No.12371302), the Key Program of the National Natural Science Foundation of China (No.12431011) and the horizontal research project (No.KFA24538).

References

- [1] Holden J, Goel N. Fast-forwarding to a future of on-demand urban air transportation[R]. San Francisco: Uber Elevate, 2016.
- [2] Thippavong D P, Apaza R, Barmore B, et al. Urban air mobility airspace integration concepts and considerations[C]//2018 Aviation Technology, Integration, and Operations Conference. 2018: 3676.
- [3] Ribeiro J K, Borille G M R, Caetano M, et al. Repurposing urban air mobility infrastructure for sustainable transportation in metropolitan cities: A case study of vertiports in São Paulo, Brazil[J]. *Sustainable Cities and Society*, 2023, 98: 104797.
- [4] Willey L C, Salmon J L. A method for urban air mobility network design using hub location and subgraph isomorphism[J]. *Transportation Research Part C: Emerging Technologies*, 2021, 125: 102997.
- [5] Ma Z, Yang X, Chen A, et al. Assessing the resilience of multi-modal transportation networks with the integration of urban air mobility[J]. *Transportation Research Part A: Policy and Practice*, 2025, 195: 104465.
- [6] Shao Q, Shao M, Lu Y. Terminal area control rules and eVTOL adaptive scheduling model for multi-vertiport system in urban air Mobility[J]. *Transportation Research Part C: Emerging Technologies*, 2021, 132: 103385.
- [7] Fadhil D N. A GIS-based analysis for selecting ground infrastructure locations for urban air mobility[D]. Ingolstadt: Technical University of Munich, 2018.
- [8] Lim E, Hwang H. The selection of vertiport location for on-demand mobility and its application to Seoul metro area[J]. *International Journal of Aeronautical and Space Sciences*, 2019, 20: 260-272.
- [9] Jeong J, So M, Hwang H Y. Selection of vertiports using K-means algorithm and noise analyses for urban air mobility (UAM) in the Seoul metropolitan area[J]. *Applied Sciences*, 2021, 11(12): 5729.
- [10] Daskilewicz M, German B, Warren M, et al. Progress in vertiport placement and estimating aircraft range requirements for eVTOL daily commuting[C]//2018 Aviation Technology, Integration, and Operations Conference. 2018: 2884.
- [11] Rath S, Chow J Y J. Air taxi skyport location problem with single-allocation choice-constrained elastic demand for airport access[J]. *Journal of Air Transport Management*, 2022, 105: 102294.
- [12] Chen L, Wandelt S, Dai W, et al. Scalable vertiport hub location selection for air taxi operations in a metropolitan region[J]. *INFORMS Journal on Computing*, 2022, 34(2): 834-856.
- [13] Shin H, Lee T, Lee H R. Skyport location problem for urban air mobility system[J]. *Computers & Operations Research*, 2022, 138: 105611.
- [14] Wei L, Justin C Y, Mavris D N. Optimal placement of airparks for STOL urban and suburban air mobility[C]//AIAA Scitech 2020 Forum. 2020: 0976.
- [15] Zhang H, Feng D, Zhang X, et al. Urban Logistics Unmanned Aerial Vehicle Vertiports Layout Planning[J]. *Journal of Transportation Systems Engineering and Infor-*

- mation Technology, 2022, 22(3): 207-214.
- [16] O’Kelly M E. The location of interacting hub facilities[J]. *Transportation Science*, 1986, 20(2): 92-106.
 - [17] Campbell J F. Integer programming formulations of discrete hub location problems[J]. *European Journal of Operational Research*, 1994, 72(2): 387-405.
 - [18] Sangaiah A K, Khanduzi R. Tabu search with simulated annealing for solving a location-protection-disruption in hub network[J]. *Applied Soft Computing*, 2022, 114.
 - [19] Wandelt S, Dai W, Zhang J, et al. Toward a Reference Experimental Benchmark for Solving Hub Location Problems[J]. *Transportation Science*, 2022, 56(2): 543-564.
 - [20] Alumur S A, Campbell J F, Contreras I, et al. Perspectives on modeling hub location problems[J]. *European Journal of Operational Research*, 2021, 291(1): 1-17.
 - [21] Najy W, Diabat A. Benders decomposition for multiple-allocation hub-and-spoke network design with economies of scale and node congestion[J]. *Transportation Research Part B: Methodological*, 2020, 133: 62-84.
 - [22] Kreimeier M, Stumpf E, Gottschalk D. Economical assessment of air mobility on demand concepts with focus on Germany[C]//16th AIAA Aviation Technology, Integration, and Operations Conference. 2016: 3304.
 - [23] Samir M, Sharafeddine S, Assi C M, et al. UAV Trajectory Planning for Data Collection from Time-Constrained IoT Devices[J]. *IEEE Transactions on Wireless Communications*, 2020, 19(1): 34-46.
 - [24] Oliveira F A, de Sá E M, de Souza S R. Benders decomposition applied to profit maximizing hub location problem with incomplete hub network[J]. *Computers & Operations Research*, 2022, 142.
 - [25] Yin J, Yang L, Liang Z, et al. Real-Time Rolling Stock and Timetable Rescheduling in Urban Rail Transit Systems[J]. *INFORMS Journal on Computing*, 2025.
 - [26] Mardia K V, Kent J T, Taylor C C. *Multivariate Analysis*[M]. John Wiley & Sons, 2024.
 - [27] Johnston T, Riedel R, Sahdev S. To take off, flying vehicles first need places to land[J]. *McKinsey Center for Future Mobility*, 2020: 2-8.